Computational investigation of charge transfer mechanisms in dye-sensitized solar cells: unraveling the influence of anchoring groups in 2-styryl-5-phenylazo-pyrrole designed dyes

T. Iqbal [a], M. Sajid [b], B. F. Felemban[c], H.T. Ali[c], A.B. Suriani[d], K. Ali [a,*]
[a] *Nano-optoelectronics Research Laboratory, Department of Physics, University of Agriculture Faisalabad, 38040, Pakistan*
[b] *Institute of Micro-Nano Optoelectronics, Optical Engineering, Shenzhen University. China*
[c] *Department of Mechanical Engineering, College of Engineering, Taif University, Taif 21944, Kingdom of Saudi Arabia*
[d] *Department of Physics, Faculty of Science and Mathematics, Universiti Pendidikan Sultan Idris, 35900 Tanjung Malim, Perak, MALAYSIA*

The proposed dyes demonstrated characteristics conducive to achieving high-power conversion efficiency (PCE) in dye-sensitized solar cells (DSSCs). Novel azo dyes diverse anchoring groups, including carboxylic acid, carboxylic diacid, biscarbodithiolic acid, phosphonic acid, and sulfonic acid, were examined to assess their impact on electronic and optical properties within DSSCs. A computational investigation was conducted to design and evaluate charge transfer mechanisms using azo-pyrrole-based dyes for DSSCs performed with the Gaussians 09 and employing TD-DFT techniques with functions like B3LYP and a 6-31G (d, p) basis set to analyze ground and excited state characteristics. Enhanced charge transfer was observed due to improved molecular properties within DSSCs. The analysis encompassed electronic and optical properties, UV-Vis absorption spectra, light harvesting efficiency, and hardness to elucidate the effects of various anchoring groups. Carboxylic acid-based dyes exhibited broad absorption spectra, the longest maximum wavelength, and the highest light harvesting efficiency, indicating proficient electron injection capabilities.

(Received September 16, 2024; Accepted January 20, 2025)

Keywords: Dye-sensitized solar cells, TD-DFT, B3LYP, Dyes, Light harvesting efficiency

1. Introduction

Solar power stands as Earth's most abundant energy source, with its conversion into electricity via photoelectrochemical solar cells widely seen as the optimal solution for addressing the global energy crisis, thanks to its vast reserves and lack of pollution [1]. Despite dominance among commercially accessible solar cells relying on inorganic silicon semiconductors, their widespread use has been constrained by the high cost of high-purity silicon. Among renewable energy technologies, nanocrystalline dye-sensitized solar cells, introduced by O'Regan and Grätzel in 1991, have captured significant consideration due to their potential for cost-effective production, environmentally friendly components, comparatively high conversion efficiencies, and versatility in manufacturing and application [2-5] PCE of DSSCs has risen from around 7% to about 14% [6]. However, the absence of considerable progress in DSSC efficiency emphasizes its fundamental difficulty, particularly as compared to comparable third-generation solar cells with conversion efficiency of 25.7% and 18%, respectively, perovskite and organic solar cells [7].

Despite the notable high efficiency achieved by solar cells utilizing ruthenium complexes and zinc porphyrins, their production faces significant challenges, including limited resources, complexity in synthetic procedures, and environmental risks [8]. To be a perfect dye for DSSCs, it

* Corresponding author: khuram_uaf@yahoo.com
https://doi.org/10.15251/JOR.2025.211.61

must have following characteristics: (1) broad absorption spectrum covering near-infrared and visible regions; (2) strong chemisorption on semiconductor surface; (3) well-aligned energy levels of its LUMO and HOMO with semiconductor CB and electrolyte redox potential to allow efficient dye regeneration and electron injection; (4) ability to suppress recombination of electrons between semiconductor and electrolyte species and (5) low tendency to aggregate, which can cause electron-hole recombination [9].

Recently, photoactive materials composed of metallic complexes containing organic ligands have been applied in solar cells due to their ability to boost solar cell photovoltaic performance by facilitating charge separation, reducing charge recombination, and having a longer average exciton diffusion length [10]. Sunlight is absorbed by dyes and facilitates charge transfer between semiconductors and electrolyte. The semiconductor electrode receives excited electrons, while the electrolyte restore oxidized dye, which in turn gathers electrons from the counter electrode to complete the circuit [11]. DSSCs operate differently than conventional solar cells by utilizing excited dye molecules for electron injection into the semiconductor's conduction band, and the reduction of dye by redox electrolyte is connected to the counter electrode [12].

In the last ten years, there has been considerable interest in materials derived from azo dyes. Azo dyes belong to a category of compounds featuring a double bond between nitrogen atoms (N double bond N). These dyes have gained widespread use within materials sensitive to organic photo activation owing to their capacity to absorb visible light rays, strong chemical stability, and great suitability for solution-based processes [13]. Recently, Mikroyannidis *et al,* have successfully synthesized new dyes utilizing 2-styryl-5-phenylazo-pyrrole as a foundation. The molecular structure of these dyes involves a substituted-phenylazo group on one side and a cyanovinylene 4-nitrophenyl group on opposite side of the pyrrole ring. In addition to widely employed carboxylic acid, various other groups, including biscarbodithiolic acid, phosphonic acid, and similar options, have been identified as acceptor groups [14]. Troisi and colleagues have conducted studies on the effectiveness of electron transfer, crucial aspects of comprehending impact of anchoring groups [15]. Conversely, diverse anchoring groups may influence the electronic and optical characteristics of dyes, a crucial feature in the advancement of dye sensitizers [16]. Currently, there is a growing interest in the investigation of dyes with larger absorption spectra, even extending into the infrared region.

This research employed density functional theory calculations to explore the impact of different groups including phosphonic acid biscarbodithiolic acid and carboxylic diacid in addition to carboxylic acid and sulfonic acid anchoring groups. The dyes under investigation featured substituted-phenylazo as one acceptor group and cyanovinylene 4-nitrophenyl as other, with pyrrole ring serving as a donor. Theoretical calculations were conducted, elucidating why and how distinct anchoring groups influence dye's functioning, specifically in terms of electron injection efficiency. A popular approach is DFT because it produces results that are close to actual observations and can be utilized to investigate producing organic dyes which are used in DSSC [17].

2. Computational method

The free dye geometries were optimized fully using B3LYP hybrid functional at DFT level of theory [18]. The optimization utilized the 6-311+G** basis set in gas phase. Computations were conducted on optimized geometries at same level. Optical absorption spectra based on optimized geometries were obtained through TD-DFT [19] calculations, employing B3LYP and range-separated functional, with 6-311+G** basis sets for calculating oscillator strengths and excitation energies of 10 lowest singlet–singlet transitions of these dyes.

Single-point computations were conducted at identical levels for cationic and anionic states of natural molecules. The optimized structure of molecule was utilized to determine quantum chemical properties. Solvent effects were carried out in tetrahydrofuran (THF) solvent, chosen for the dyes as they are soluble and stable in nonprotic solvents like THF. Experimental findings reported were conducted in THF, and in this study, all ground state calculations were executed using the Gauss View and Gaussian 09 program [20, 21].

DFT is a predominant and versatile quantum mechanical approach that is employed to calculate the electronic structure of atoms, molecules, and solids. Since the 1970s, DFT has found extensive application in computational solid-state physics. It is a method that computes the properties of a molecule by considering its electron density.

3. Results and discussion

In this current investigation, initial optimization for determining optoelectronic properties utilized B3LYP ωB97XD, MPW1PW91, CAM-B3LYP, HSEH1PBE, and PBEPBE functionalities and 6-31G (d,p) basis set. Among these methods, B3LYP/6-31G (d,p) approach within the DFT framework exhibits most significant relationship with experimental λ_{max} value. Hence it is considered the most suitable method for subsequent calculations involving designed molecules D1-D5.

DSSC is a form of third-generation PV for uncontaminated energy and affordable manufacture, optimistic for flexible and lightweight cells because they are possibly produced from many substrates like plastics, glass, and ceramic [22]. The highest solar-to-electric PCE of 11.5% has been attained [23]. Azo-photosensitizers are promising dye options in DSSC because of their high molar extinction coefficients [24]. The DSSC is often constructed of a semiconductor with a high band gap, TiO_2, which is usually sensitized with molecular dyes. Nanoporous TiO_2 serves as a dye sensitizer support, electron acceptor, and electrical conductor. We calculated the electronic structures of the investigated azo dyes using TD-DFT. This work was completed to direct future synthesis toward molecules that are more beneficial as active photovoltaic sensitizer materials.

3.1. Geometry optimization structures and geometrical parameters

With these concerns in mind, we studied the influence of various chemical structures on the optoelectronic capabilities of Azo-Pyrrole dyes based on 2-styryl-5-phenylazo-pyrrole. A variety of innovative Azo-Pyrrole-based dyes have been developed by inserting various groups, such as Sulphonic acid (D1), Carboxylic acid (D2), Carboxylic diacid (D3), Biscarbodithiolic acid (D4) and phosphonic (D5) at the bay position of azo dyes to demonstrate the rational layout of novel candidate supplies for organic solar cells.

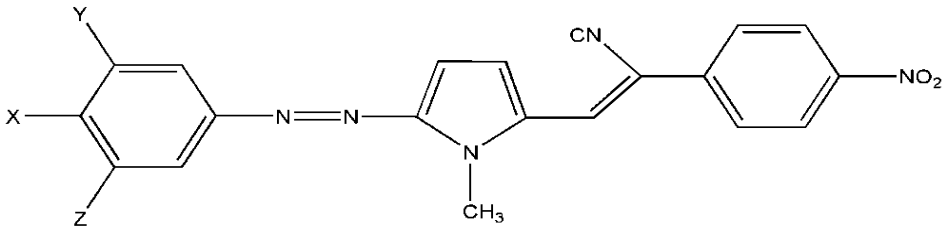

Fig. 1. Structure of investigated dyes, 2-styryl-5-phenyl azo pyrrole.

Y=H	Y=H	Y=H	Y=H	Y=COOH
X=SO_3H	X=COOH	X=H	X=CSSH	X=$P0_3H_2$
Z=H	Z=H	Z=COOH	Z=H	Z=H
D1	D3	D3	D4	D5

Different groups connect to different positions of the phenyl fragment in Azo dyes. Sulphonic acid (SOH) is connected to the X position of the phenyl fragment in D1, whereas hydrogen is linked to the Y and Z locations. Carboxylic acid (COOH) and hydrogen bind in the same place as D1 in D2. In D3, carboxylic diacid is connected at the Y and Z positions of the phenyl fragment, whereas hydrogen is bonded at the X position. Biscarbodithiolic acid (CSSH) is connected

at the X position of the phenyl fragment in D4, and hydrogen is attached at the Y and Z locations. In D5, phosphonic acid (PO_3H_2) is bonded at X and hydrogen is attached at Y and Z.

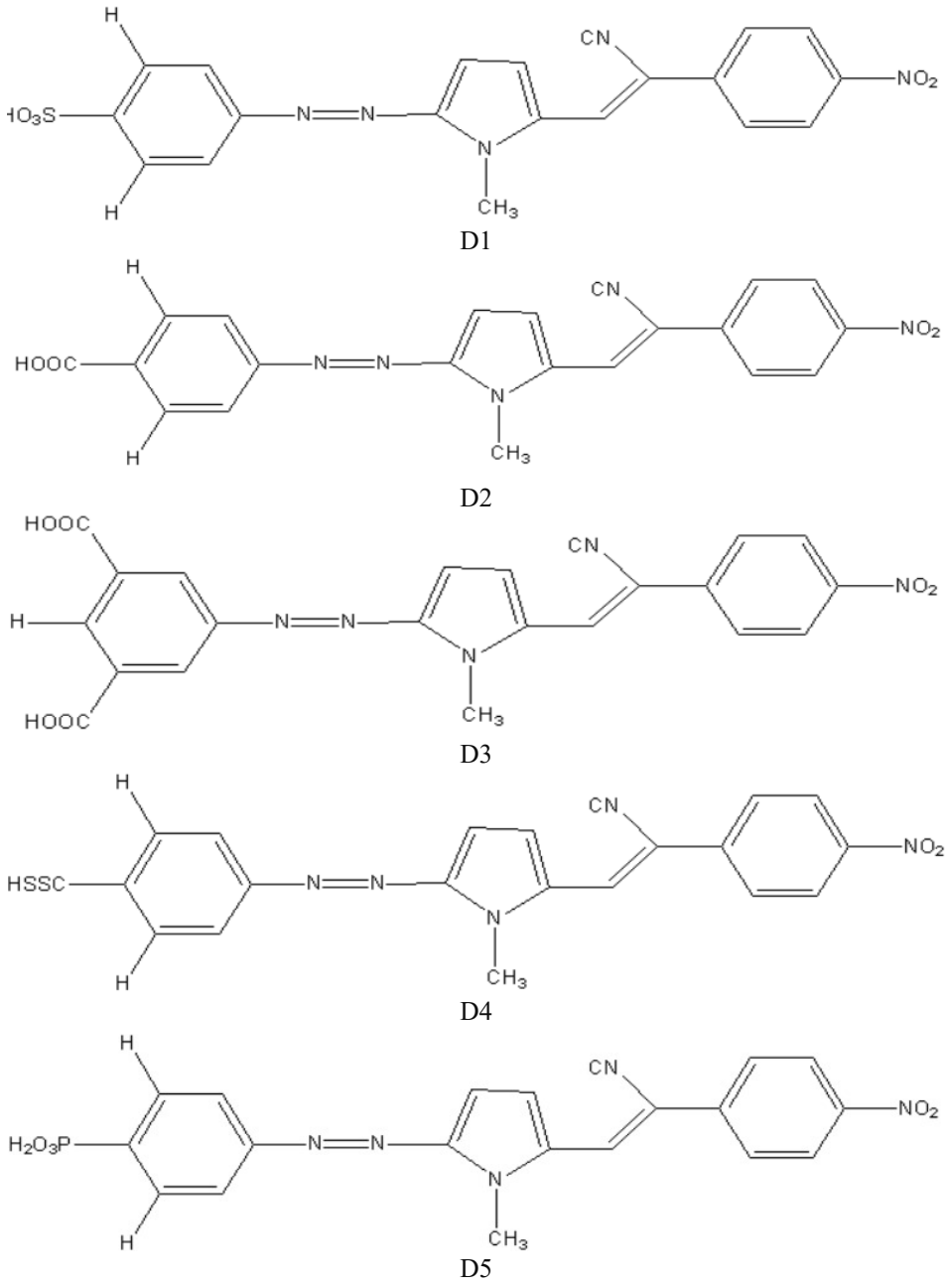

Fig. 2 Molecular structure of different investigated azo dyes.

Gaussian-09 software package was used to do free dye computations. We optimized the examined molecules DI-D5 at the ground state via planar confirmation, which aids electron delocalization via conjugation. The whole structure was optimized by B3LYP approach and 6-31G (d) basis set. The ball and stick model of the studied dyes (D1-D5) in ground state is shown in Figure 3.

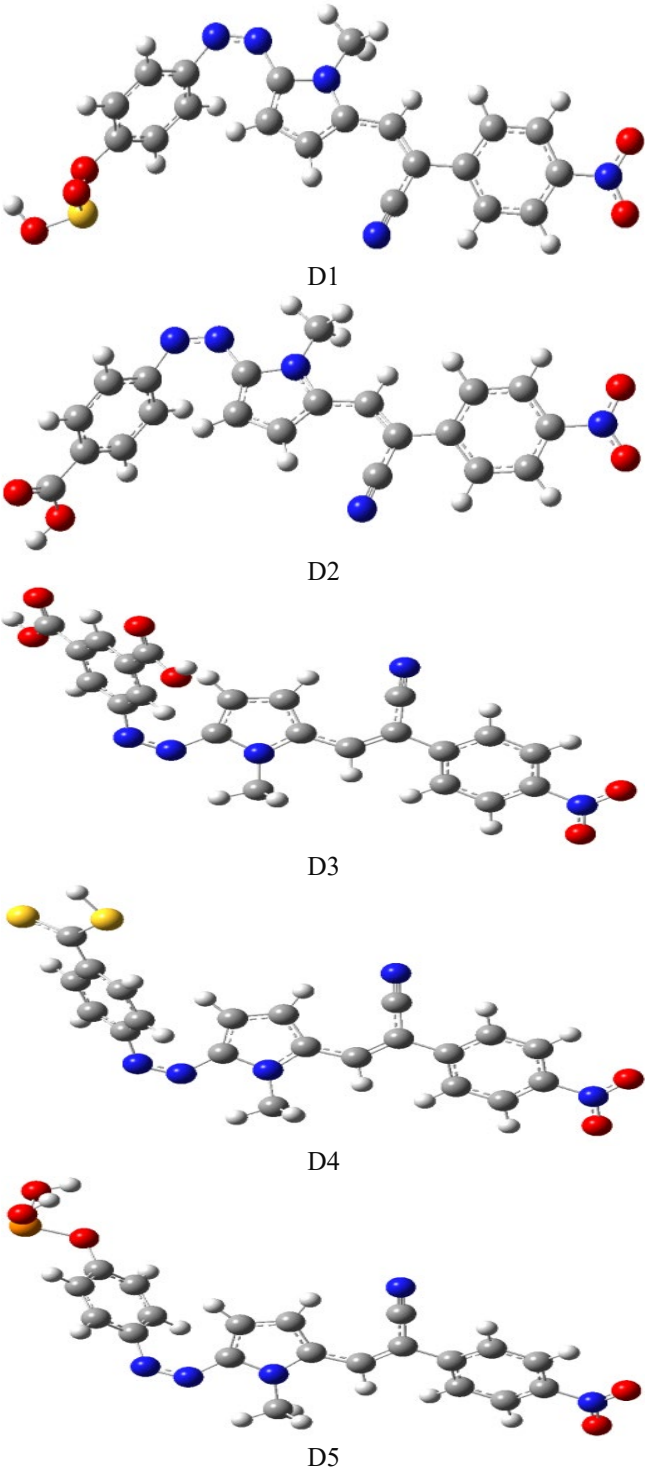

Fig. 3. Optimized structures of investigated dyes (D1, D2, D3, D4 and D5) along with Azo-Pyrrole.

3.2. Frontier molecular orbital

The advantageous electrical and optical features play an important part in achieving a greater solar-to-electricity conversion efficiency. Potential difference between HOMO and LUMO may be utilized to calculate energy gap. Theoretically, HOMO and LUMO levels were obtained in these dyes using DFT calculations on optimal structures. Table 1 also includes determined gap energy. Trend of HOMO level of investigated molecules is found as D5 > D1 > D3 > D4 > D5 while order of LUMO as D5 > D1 > D2 > D4 > D3. The trend of energy gap (E_g) values is in order of D3

> D2 > D4 > D1 >D5 as shown in the table. This trend shows that D2 has higher HOMO and D3 has higher LUMO values.

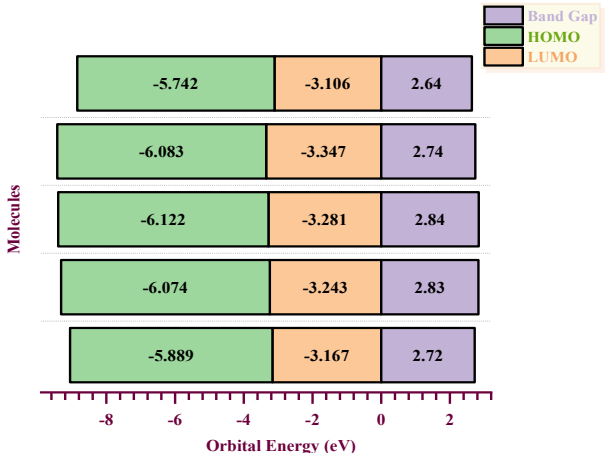

Fig. 4. Calculated energy level diagram of dyes at B3LYP/6-31G (d, p) level.

Fig.4 depicts an energy level of dye with higher occupied molecular orbitals and lower unoccupied molecular orbitals. According to B3LYP technique results, maximum absorbance (λ_{max}) for dyes is in a sequence of 1 (D2) > 2 (D4) > 3 (D1) > 4 (D5) >5 (D3).

Table. 1 Calculated E_{HOMO}, E_{LUMO}, and E_{HOMO} - E_{LUMO} gaps of all designed dyes at B3LYP/6-31G (d,p).

Dye	E_{HOMO}	E_{LUMO}	$E_{HOMO} - E_{LUMO}$ (Band Gap)
D1	-5.889	-3.167	2.722
D2	-5.742	-3.106	2.636
D3	-6.122	-3.281	2.841
D4	-6.083	-3.347	2.736
D5	-6.074	-3.243	2.831

Thus, we found that dye D2 has a lower energy gap corresponding to other dyes. DI has a lower energy gap than D3. The sulfonic acid (SO_3H) does not raise the HOMO energy of the corresponding dye (D1). However, the HOMO level of D2 (-5.742) eV is greater than other dyes. Therefore, the acid group (COOH) for D2 is effective in raising HOMO energy levels of corresponding dye.

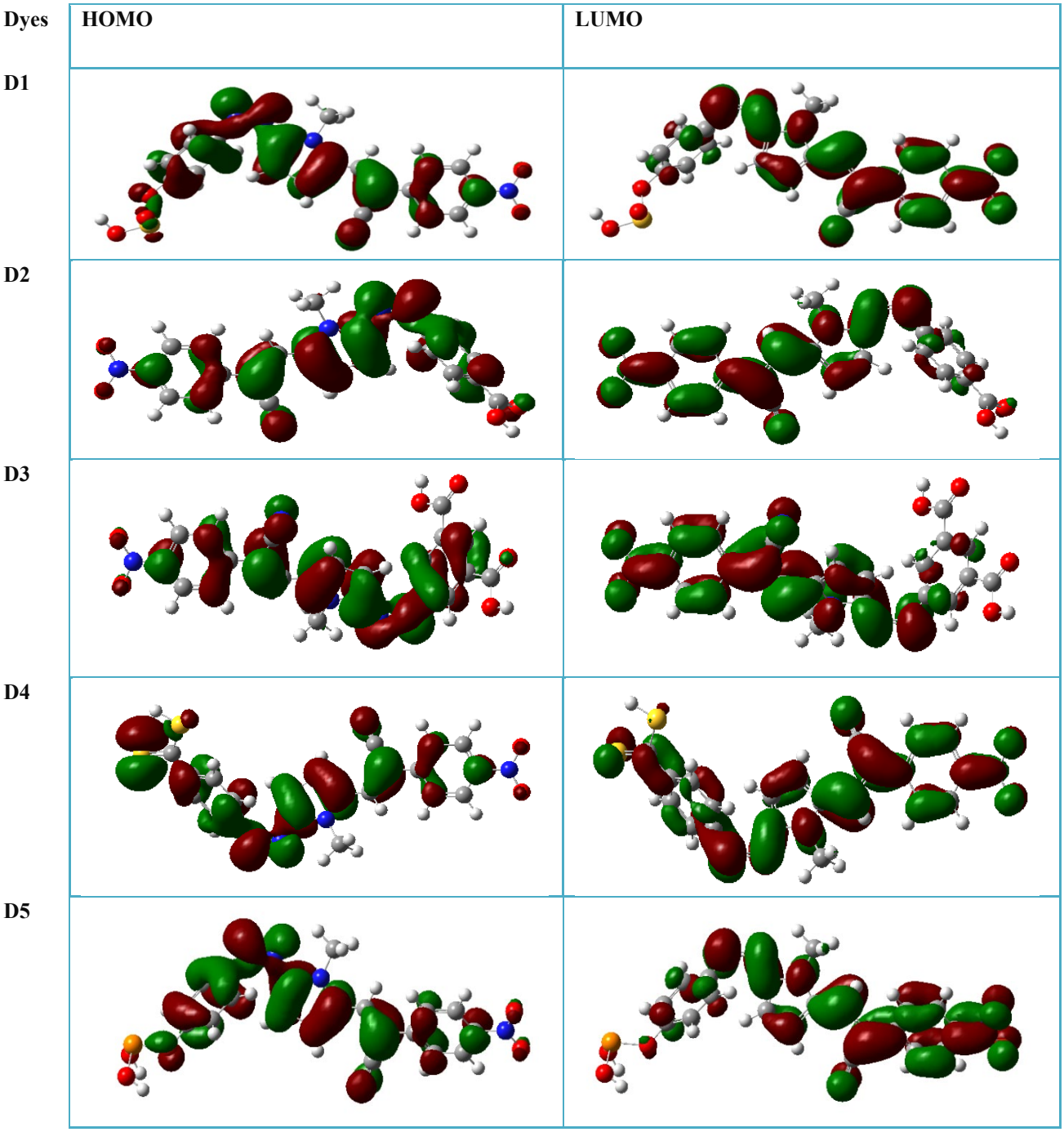

Fig. 5. Frontier molecular orbitals at ground state of dyes calculated at B3LYP/6-31G (d,p) level of theory.

FMO distribution patterns are important for distinguishing the optoelectronic properties of dyes. Thus, the FMO substituted molecules are also studied, and the spatial distribution of HOMO LUMO orbitals of designed dyes. Designed dyes FMO which indicate great intersection in HOMO and LUMO and strong optical adsorption. The groups of SOH, COOH, $(COOH)_2$, (CSSH), and (PO_3H_2) at different positions can significantly vary the HOMO, LUMO, and E_g values of Azo Pyrrole.

The optoelectronic properties of investigated dyes can be identified by analyzing the distribution pattern of frontier molecular orbital FMOS assembled. As shown in the FMO diagram (fig. 5), in HOMO and LUMO of D1, D2, D3, D4 and D5 delocalization of electron density is at SOH, COOH, 2(COOH), (CSSH) and (PO_3H_2) i-e. Donor, so we can predict that the transition in

D1, D2, D3, D4, and D5 are intermolecular charge transfer ICT. In dyes D1, D2, D3, D4 and D5, charge density is delocalized on the whole molecule in HOMO and LUMO so can be predicted to show transition.

The calculated findings indicate that energy level at HOMO of each of these dyes are less compared to I/I_3^- electrolyte's reduction potential energy (4.8 eV), suggesting that the electrons lose by dyes might be restored by receiving electrons by electrolyte, whereas energy levels at LUMO of dyes are greater than TiO_2 CB edge (-4.1 eV) [24]. It implies that LUMO values of all five dyes must be able to pump electrons into TiO_2 conduction band.

Figure 5 shows an energy level diagram of dye HOMO and LUMO for dyes D1-D5. Results of the B3LYP technique demonstrate that the maximum absorbance for dyes is in the order of (D2) > (D3) > (D4) > (D1) > (D5).

3.3. Optical and electronic properties

The anchoring group, as an inherent feature, might influence electron transfer through electronic interaction between semiconductor and dye [25]. Efficacy of electron transfer may affect J_{sc}, which is a critical element influencing the efficacy of DSSCs. This indicates that as the quantity of charge injected in TiO_2 surface grows, so does short-circuit density [26]. Improving J_{sc} is an efficient approach to increasing the efficiency of DSSCs [27]. This equation may be used to calculate the LHE efficiency of a dye, which is a feature linked to J_{sc},

$$LHE = 1 - 10^{-A} = 1 - 10^{-f},$$

where A (f) is dye absorption i.e., oscillator strength corresponding to λ_{max}. Higher LHE values, greater light catching. Improving the LHE might improve J_{sc}.

Table 2. Calculated λ_{max} (nm), EBE (eV), oscillator strengths (f), and light-harvesting efficiency (LHE) of dyes 1–5 with the B3LYP method.

Dyes	**λ_{max} (nm)**	**EBE (eV)**	***F***	**LHE**
D1	417.04	0.4843	0.3416	0.5446
D2	422.31	0.5227	0.4276	0.6264
D3	419.22	0.4995	0.2663	0.4584
D4	415.04	0.5280	0.2591	0.4493
D5	390.94	0.4501	0.2535	0.4422

According to table 2, dye 2 has higher oscillation strength (f) and a greater LHE than other dyes. As the LHE of different dyes is examined, it is obvious that a dye constructed from Carboxylic acid (-COOH) has a greater LHE and a wider absorption spectrum than other dyes. Suggests that a dye composed of carboxylic acid has a greater electron-depleting capability of the anchoring group, resulting in a stronger oscillator, better LHE, and more efficient light-harvesting capabilities.

Results obtained for values of LHE, and EBE of dye 2 demonstrate that dye 2 may be an efficient structure for electron injection when compared to other dyes. Specifically, carboxylic acid might be an appealing anchoring group utilized for building a dye with an excellent rate of electron transfer from sensitizer to semiconductor. In contrast, electron lowest unoccupied molecular orbital (ELUMO) values for dyes listed in Table 2 indicate that ELUMO closely aligns with conduction band (CB) of TiO_2 in dye 2 when compared to other dyes.

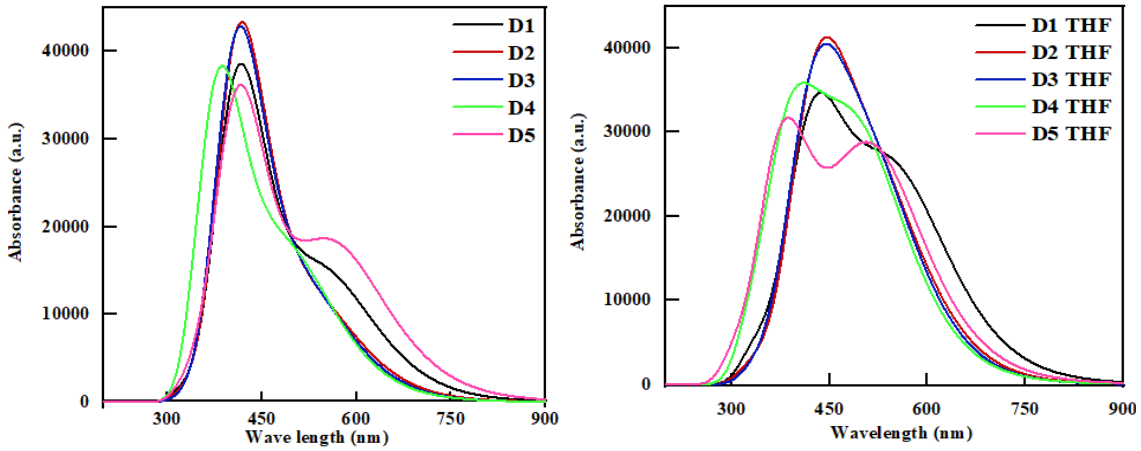

Fig. 6. Simulated absorption spectra of D1, D2, D3, D4 and D5 at the B3LYP/6-311þG (d, p) level.

3.4. Electronic and optical properties of deprotonated dyes

Generally, when dye adheres the surface of semiconductor, anchoring group releases the proton and binds towards semiconductor as a deprotonated dye. Table 3 represents the values of λ_{max}, EBE, oscillator strength (*f*), and LHE of deprotonated dyes. Deprotonated dyes exhibit smaller λ_{max} values compared to their associated neutral molecules, but the sequence of λ_{max} remains similar to that of neutral molecules. Specifically, dye 2 has the highest λ_{max} at 446.73 nm, followed by dye 3 at 445.46 nm, dye 1 at 437.16 nm, dye 4 at 410.03 nm, and dye 5 at 389.76 nm. Consequently, there exists an inverse relation between E_g and maximum absorption wavelengths of dyes.

Table 3. Calculated λ_{max} (nm), EBE (eV), oscillator strength (f), and LHE of dyes 1-5 with B3LYP/6-311+G method in THF.

Dyes	λ_{max} (nm)	EBE (eV)	*F*	LHE
B3LYP				
D1	437.16	0.4996	0.5674	0.7292
D2	446.73	0.4840	0.6647	0.7835
D3	445.46	0.4860	0.5168	0.6957
D4	410.03	0.5143	0.6454	0.7740
D5	389.76	0.5062	0.4885	0.6752

To assess charge separation in these dyes, EBE for dyes was determined. It plays an important part in the functioning of DSSCs as it governs charge separation in solar cells. Higher EBE in a dye leads to reduced charge separation efficacy.

It is defined as a disparity between the energy of electrical and optical band gaps. The energy difference between HOMO and LUMO levels is referred to as electronic band gap, while the optical gap is estimated as initial excitation energy [28]. The computed EBE of these dyes is presented in following order: 4 (-CSSH) > 5 (-PO_3H_2) > 1 (-SO_3H) > 3 (-2COOH) > 2 (-COOH). This indicates that dye 2 possesses the smallest EBE and is highly advantageous for efficient light-to-electricity conversion of energy through the separation of a bound exciton. Additionally, lower EBE values for dyes 3 and 1 suggest that exciton may split more effectively in these dyes compared to the others.

According to the findings, EBE and λ_{max} have an inverse relationship, which means that dyes with less exciton binding energy have greater λ_{max} and longer excited state lifetime (or greatest absorption behavior). According to findings, carboxylic acid (-COOH) dyes should have the lowest E_g, EBE, and highest maximum absorbance (λ_{max})

Furthermore, DOS analysis of all proposed molecules (D1-D5) was done using B3LYP/6-31G (d, p), which contributed to understanding their optoelectronic capabilities and describing

impact of each fragment on electronic charge density. DOS analysis determines E_g and HOMO-LUMO energy levels determined by FMO analysis. DOS graph illustrates positive and negative energy values in eV that represent bonding and anti-bonding orbitals engaged in charge distribution around dye molecules, respectively, while zero signifies the absence of bonding orbital interaction.

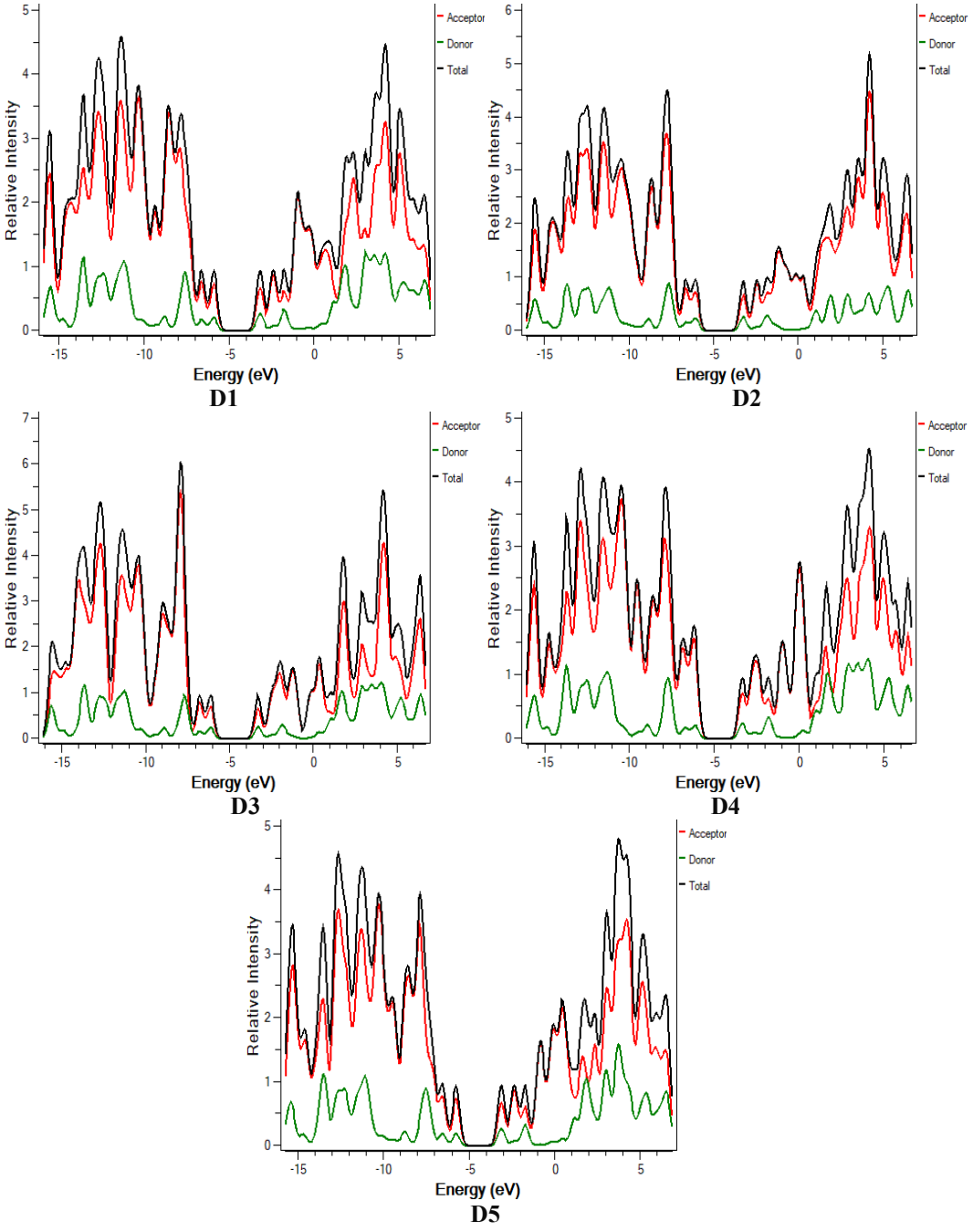

Fig. 7. Density of State of investigated dyes (D1-D5).

In the DOS graph, negative values on the x-axis correspond to HOMO energies, while positive values represent LUMO energies. In the context of D1-D5, the donor units exhibit their highest electron density distribution around HOMO, ranging from -10 eV to -5eV, while the acceptor units display their greatest electron density distribution around LUMO, spanning from -2 to 5 eV.

This implies that intramolecular charge is transferred from HOMO to LUMO. The central donor contributes 72%, 75.4%, 48.5%, and 73.9% to HOMO for D1-D5, respectively, whereas the acceptor moieties contribute 52.2%, 48.7%, 45.3%, and 85.8% to LUMO for D1-D5.

According to Figure 7, the LUMO energies of all created molecules vary from 3.10 to 3.34 eV and the HOMO values range from 5.74 to 6.12 eV. The HOMO-LUMO energy gap determined from DOS and FMO is the identical since they are analogues. The newly created molecules (D1-D5) can be regarded as an optimistic contender for building efficient DSSCs based on the foregoing discussion since they have the smallest HOMO-LUMO energy gap.

3.5. Molecular Parameter

To validate the findings of the study, a theoretical methodology was employed to establish a link between the efficiency of five tested dyes and their electronic properties. The objective was to assess the feasibility of utilizing quantum-mechanical outcomes in evaluating the efficiency of these dyes. Quantum results were obtained for all five dyes. Calculations were employed to determine quantum-chemical specifications for synthesized organic compounds, including energy levels of higher occupied molecular orbital (E_{HOMO}) and lower unoccupied molecular orbital (E_{LUMO}). Additionally, specific parameters such as absolute softness (σ), absolute hardness (η), electrophilicity index (ω), and absolute electronegativity (χ), were both measured and calculated. Equations (1–4) were utilized in the computation of molecular parameters, as outlined below. $\sigma = \frac{1}{\eta}$

$$\eta = \frac{E_{LUMO} - E_{HOMO}}{2}$$

$$\omega = \frac{\chi^2}{2\eta}$$

$$\chi = -\frac{(E_{HOMO} - E_{LUMO})}{2}$$

Table 4. Quantum chemical parameters of dyes.

Dyes	σ	η	ω	χ
D1	0.732	1.370	7.510	4.533
D2	0.759	1.318	7.424	4.424
D3	0.704	1.420	7.781	4.701
D4	0.731	1.368	8.125	4.715
D5	0.707	1.415	7.660	4.658

a. Calculating molecules stability and reactivity requires an understanding about absolute softness (σ) and hardness (η). Hard molecule has a significant energy gap, whereas soft molecule has relatively little energy. Soft molecules have higher reactivity than hard molecules because they may give electrons to acceptors more readily.

b. Short HOMO-LUMO gap indicates significant chemical reactivity. It is noted that energy separation between HOMO and LUMO symbolizes the molecule's chemical hardness. Table 4.4 shows that increasing the hardness (η) of molecule increases its stability, as per the concept of maximal hardness. Chemical hardness values of compounds are observed in the following order: D3(1.420) > D2(1.415) > D1(1.370) > D4(1.368) > D5(1.318)

c. Electrophilicity index (ω) determines molecule capacity to take electrons. Outcomes of this parameter follow the sequence: D4 (8.125) > D3 (7.781) > D2 (7.660) > D1 (7.510) > D5 (7.424).

d. The energy gap (E_{HOMO}–E_{LUMO}) works as a key stability indicator. It can be utilized as an essential measure in determining chemical molecular reactivity. So ft molecule is more polarized and has a smaller energy gap.

3.5. Transition density matrix and exciton binding energy

TDM study evaluates and interpret electronic transition processes in DSSCs. Graph depict unique 3D map among two Eigen states of recently developed chemicals. It shows the distribution of associated electron-hole pairs, allowing them to determine durations of coherence and delocalization. They are mostly used to describe excitations caused by charge transport within solar cells. Absorption of dye molecules (D1-D5) upto six excitation states was investigated using B3LYP/6-31G (d,p) functional and Multiwfn 3.7 software. Influence of hydrogen was ignored because of little impact of hydrogen atoms. TDM findings are displayed in Figure 8.

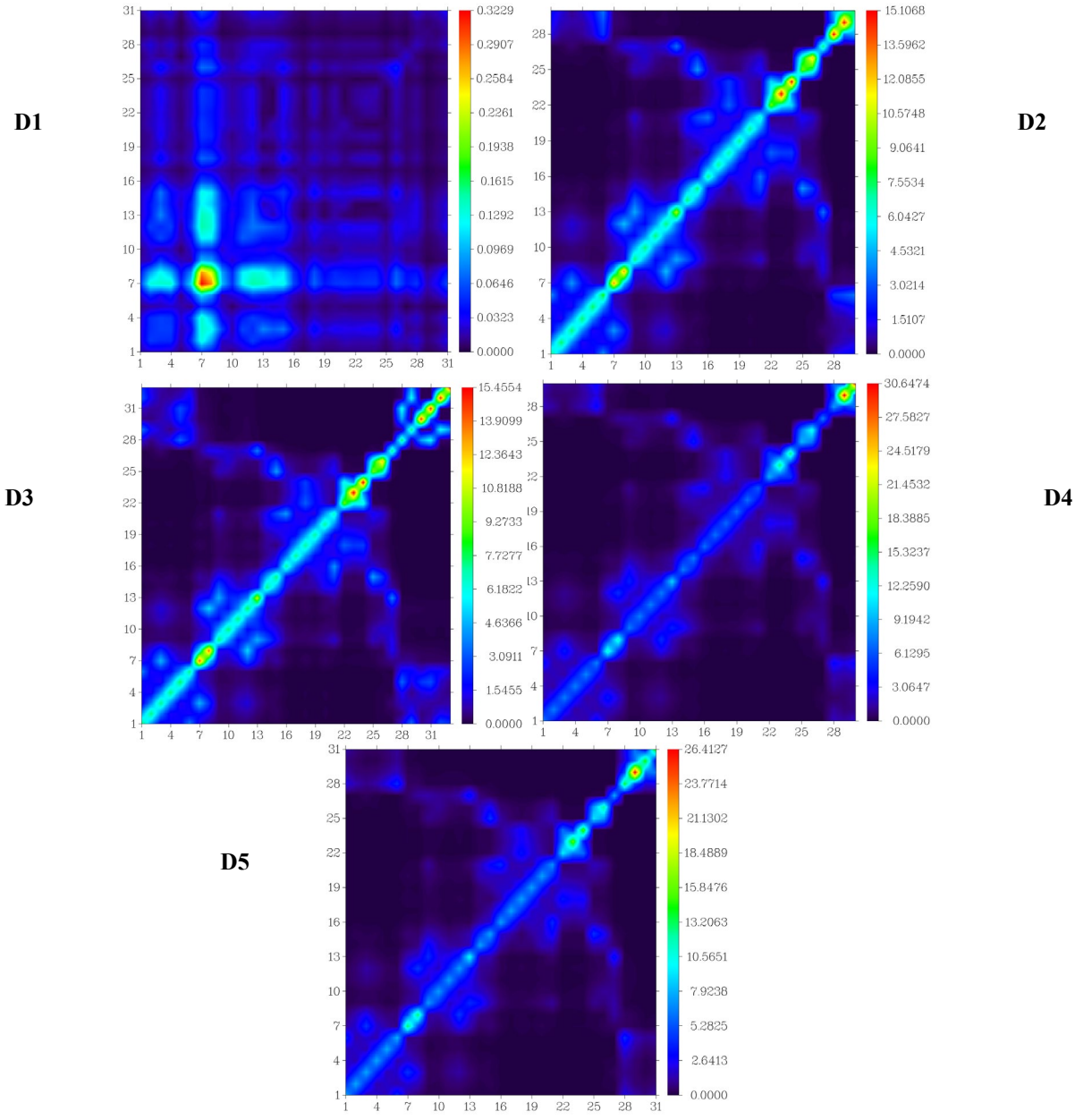

Fig. 8. Stimulated TDM of designed molecules D1-D5.

4. Conclusion

This study presents a comprehensive computational investigation into design and evaluation of azo-pyrrole-based dyes for DSSCs. The study explores impact of several anchoring groups, on optical and electrical properties of dyes. Theoretical calculations, employing DFT with B3LYP/6-31G (d, p), were carried out to assess charge transfer and performance of these dyes. The investigation reveals that choice of anchoring group significantly influences the properties of dyes. Among the tested anchoring groups, carboxylic acid-based dye exhibits longest maximum absorption wavelength, widest absorption spectra, and highest LHE, suggesting its potential for efficient electron injection. Computational results show an enhancement in charge transfer, leading to improved properties of the molecules in DSSCs. Furthermore, the study includes a detailed analysis of electronic properties, frontier molecular orbitals, energy gaps, and light-harvesting efficiencies of designed dyes. carboxylic acid as anchoring group demonstrate favorable characteristics, making them promising candidates for use in DSSCs. Additionally, the article discusses quantum chemical parameters, such as absolute softness, absolute hardness, electrophilicity index, and electronegativity to evaluate the stability, reactivity, and electron-accepting ability of dyes. Findings suggest that carboxylic acid-based dye exhibits favorable quantum chemical parameters, further supporting its potential as an efficient sensitizer for DSSCs. Results highlight the significance of anchoring groups in influencing optoelectronic properties of dyes, paving way for development of effective dye sensitizers for future solar cell application.

Acknowledgments

The authors extend their appreciation to Taif University, Saudi Arabia, for supporting this work through project number (TU-DSPP-2024-321).

The authors also thank Higher Education Commission (HEC) of Pakistan [Grant No: 8615/Punjab/NRPU/R&D/HEC/2017] and Prof. Khurshid Ayub, COMSATS University Islamabad, Pakistan for their support.

Funding

This research was funded by Taif University, Saudi Arabia, Project No. (TU-DSPP-2024-321).

Data availability statements

The data supporting this study's findings are available from the corresponding author upon reasonable request.

References

[1] Akram, M., et al., Computational and Theoretical Chemistry, 2021. 1201: p. 113242; https://doi.org/10.1016/j.comptc.2021.113242

[2] Modelli, A., P.D. Burrow, The Journal of Physical Chemistry A, 2011. 115(6): p. 1100-1107; https://doi.org/10.1021/jp110813f

[3] Xu, J., et al., Spectrochimica Acta Part A: Molecular and Biomolecular Spectroscopy, 2011. 78(1): p. 287-293; https://doi.org/10.1016/j.saa.2010.10.008

[4] Grätzel, M., Journal of Photochemistry and Photobiology A: Chemistry, 2004. 164(1-3): p. 3-14; https://doi.org/10.1016/j.jphotochem.2004.02.023

[5] Maqsood, S., et al., Ceramics International, 2023. 49(23): p. 37118-37126; https://doi.org/10.1016/j.ceramint.2023.08.313

[6] Lee, C.-P., C.-T. Li, and K.-C. Ho, Materials today, 2017. 20(5): p. 267-283; https://doi.org/10.1016/j.mattod.2017.01.012

[7] Khir, H., et al., Ceramics International, 2023. 49(11): p. 17620-17628; https://doi.org/10.1016/j.ceramint.2023.02.128

[8] Wu, Y. and W. Zhu, Chemical Society Reviews, 2013. 42(5): p. 2039-2058; https://doi.org/10.1039/C2CS35346F

[9] Ooyama, Y., Y. Harima, European Journal of Organic Chemistry, 2009. 2009(18): p. 2903-2934; https://doi.org/10.1002/ejoc.200900236

[10] Kerraj, S., et al., Computational and Theoretical Chemistry, 2022. 1209: p. 113630; https://doi.org/10.1016/j.comptc.2022.113630

[11] Weerasinghe, J., et al., Solar Energy, 2021. 215: p. 367-374; https://doi.org/10.1016/j.solener.2020.12.044

[12] Dissanayake, M., et al., Journal of Photochemistry and Photobiology A: Chemistry, 2012. 246: p. 29-35; https://doi.org/10.1016/j.jphotochem.2012.06.023

[13] Mikroyannidis, J., et al., Solar energy materials and solar cells, 2010. 94(12): p. 2318-2327; https://doi.org/10.1016/j.solmat.2010.08.001

[14] Pellegrin, Y., et al., Journal of Photochemistry and Photobiology A: Chemistry, 2011. 219(2-3): p. 235-242; https://doi.org/10.1016/j.jphotochem.2011.02.025

[15] Ambrosio, F., N. Martsinovich, A. Troisi, The journal of physical chemistry letters, 2012. 3(11): p. 1531-1535; https://doi.org/10.1021/jz300520p

[16] Yang, L.-N., et al., Dyes and Pigments, 2013. 99(1): p. 29-35; https://doi.org/10.1016/j.dyepig.2013.04.015

[17] Estrella, L.L., S.H. Lee, D.H. Kim, Dyes and Pigments, 2019. 165: p. 1-10; https://doi.org/10.1016/j.dyepig.2019.02.002

[18] Kusama, H., H. Orita, H. Sugihara, Solar energy materials and solar cells, 2008. 92(1): p. 84-87; https://doi.org/10.1016/j.solmat.2007.09.004

[19] Jacquemin, D., B. Mennucci, C. Adamo, Physical chemistry chemical physics, 2011. 13(38): p. 16987-16998; https://doi.org/10.1039/c1cp22144b

[20] Zare, K., N. Shadmani, Journal of Nanostructure in Chemistry, 2013. 3: p. 1-6; https://doi.org/10.1186/2193-8865-3-72

[21] Young, E.D., A. Galy, Reviews in Mineralogy and Geochemistry, 2004. 55(1): p. 197-230; https://doi.org/10.2138/gsrmg.55.1.197

[22] Hall, L.H., L.B. Kier, Journal of Chemical Information and Computer Sciences, 1995. 35(6): p. 1039-1045; https://doi.org/10.1021/ci00028a014

[23] Chen, L.M., et al., Advanced materials, 2009. 21(14-15): p. 1434-1449; https://doi.org/10.1002/adma.200802854

[24] Mikroyannidis, J., et al., Journal of Power Sources, 2011. 196(8): p. 4152-4161; https://doi.org/10.1016/j.jpowsour.2010.12.038

[25] Periyasamy, K., et al., Journal of Electronic Materials, 2023. 52(4): p. 2525-2543; https://doi.org/10.1007/s11664-023-10210-6

[26] Mikroyannidis, J.A., et al., The Journal of Physical Chemistry C, 2010. 114(3): p. 1520-1527; https://doi.org/10.1021/jp910467c

[27] Zhang, J., et al., Journal of Materials Chemistry, 2012. 22(2): p. 568-576; https://doi.org/10.1039/C1JM13028E

[28] Zhang, C.-R., et al., International journal of molecular sciences, 2013. 14(3): p. 5461-5481; https://doi.org/10.3390/ijms14035461